Available online at www.isr-publications.com/jmcs
J. Math. Computer Sci., 17 (2017), 84–95
Research Article

Online: ISSN 2008-949x

Journal of Mathematics and Computer Science

Journal Homepage: www.tjmcs.com - www.isr-publications.com/jmcs

Thermal boundary layer analysis of nanofluid flow past over a stretching flat plate in different transpiration conditions by using DTM-Padé method

Majeed A. Yousif[a], M. Hatami[b,*], Bewar A. Mahmood[c], M. M. Rashidi[d,e]

[a]*University of Zakho, Faculty of Science, Department of Mathematics, International Road Zakho-Duhok, P. O. Box 12, Duhok, Kurdistan Region, Iraq.*

[b]*Mechanical Engineering Department, Esfarayen University of Technology, Esfarayen, North Khorasan, Iran.*

[c]*University of Duhok-Faculty of Science, Department of Mathematics, Kurdistan Region, Iraq.*

[d]*Shanghai Key Lab of Vehicle Aerodynamics and Vehicle Thermal Management Systems, Tongji University, Address: 4800 Cao An Rd., Jiading, Shanghai 201804, China.*

[e]*ENN-Tongji Clean Energy Institute of Advanced Studies, Shanghai, China.*

Abstract

In this paper, Differential Transformation Method (DTM) is applied on governing equations of heat and fluid flow for a nanofluid over a horizontal flat plate. After obtaining the governing equations and solving them by DTM, the accuracy of results is examined by fourth order Runge-kutta numerical method. Due to infinite boundary condition for the stretching plate, outcomes need to an improvement method to be converged. For this aim, Padé approximation is applied on the obtained results which [10,10] Padé order had the best accuracy compared to numerical method. The influence of relevant parameters such as the transpiration parameter on temperature and nanoparticle concentration profile is discussed and it is concluded that by increasing this parameter, nanoparticles concentration over the plate decrease due to more fluid penetration from pores and this is the main reason of lower thermal boundary layer caused by fewer nanoparticles over the plate.

Keywords: Nanofluid, DTM-Padé, boundary layer, Lewis number, heat transfer.
2010 MSC: 76D10, 35Q35, 80M25.

1. Introduction

Nowadays, nanofluids are the most important topics for the researchers due to their high application in industry and technology for facility of many phenomena such as heat transfer [1–5]. Based on Aziz [6] study, Dogonchi et al. [7], Domairry and Aziz [8] and Domairry and Hatami [9] applied the mathematical methods for solving the mechanical engineering problems such as nanoparticles or particles motion modeling. Ellahi et al. [10] in a mathematical modeling, investigated the shape effect of nanosize Cu particles on the entropy generation. Also, Ellahi et al. [12] in another study analyzed the shape effect of nanoparticles suspended in HFE-7100. Mathematical modeling is widely used by the researchers

*Corresponding author
Email address: m.hatami2010@gmail.com (M. Hatami)

doi:10.22436/jmcs.017.01.08

Received 2016-11-22

[13, 14, 16–36] in the last years due to its simplicity, high accuracy and applicability in a wide range of engineering problems such as mechanical engineering, electrical engineering, chemical engineering, etc. Rana et al. [37] investigated the flow and heat transfer of a nanofluid over a nonlinearly stretching sheet by numerical solution. After that, Rashidi et al. [38–42] considered the nanofluid flow over a stretching porous plate and analyzed it by analytical and mathematical methods. Shaoqin and Huoyuan [15] used the mathematical least square method for incompressible magneto-hydrodynamic equation while Ellahi et al. [11] analyzed the mixed convection over a permeable wedge mathematically. Collocation is another mathematical technique for problem modeling which is used by Stern and Rasmussen [43] for their modeling. The nanofluid slip flow within circular concentric pipes has been theoretically investigated in the presence of thermal conditions of either constant heat flux at the outer wall and the inner wall insulated or vice versa by Turkyilmazoglu [44, 45]. Turkyilmazoglu [44] solved momentum and energy equations of nanofluids analytically to deduce the flow and heat transport phenomena in two theoretical cases, single phase and multi-phase. When the nanoparticles are uniformly distributed across the condensate boundary layer called it single phase and when the concentration of nanoparticles through the film is allowed to vary from the wall to the outer edge of the condensate film in the light of modified Buongiorno's nanofluid model named multi-phase. Zeeshan et al. [46] analyzed the effect of magnetic dipole on viscous ferro-fluid past a stretching surface with thermal radiation and show the effects of magnetic field on the particles treatment.

Comparison of the single and two-phase modeling for the nanofluids has been considered by the researchers. For instance, Haghshenas Fard et al. [21] compared the results of the single phase and two-phase numerical methods for nanofluids in a circular tube. They reported that for Cu-water the average relative error between experimental data and CFD results based on single-phase model was 16% while for two-phase model was 8%. In another numerical study, Göktepe et al. [20] compared these two models for nanofluid convection at the entrance of a uniformly heated tube which found the same results and confirm the accuracy of two-phase modeling. Mohyud-Din et al. [34] in an analytical study, considered the three dimensional heat and mass transfer with magnetic effects for the flow of a nanofluid between two parallel plates in a rotating system. As one of their main outcomes, thermophoresis and Brownian motion parameters are directly related to heat transfer but are inversely related to concentration profile. Also they found that the higher Coriolis forces decrease the temperature boundary layer thickness. Three-dimensional flow of nanofluids under the radiation (due to solar or etc.) has been analyzed by Hayat et al. [31] and Khan et al. [32]. They also computed and examined the effects of different parameters on the velocity, temperature, skin friction coefficient and Nusselt number of nanofluid flow.

Nomenclature

α_m	thermal diffusivity	q_m	wall mass flux
a	constant	q_w	wall heat flux
n	stretching parameter	D_B	Brownian diffusion confident
C	nanoparticle volume fraction	D_T	thermophoretic diffusion coefficient
Nt	thermophoresis parameter	u_w	velocity of stretching sheet
C_w	nanoparticle volume fraction	$f(\eta)$	dimensionless stream function
C_∞	ambient nanoparticle volume fraction	$g(\eta)$	gravitational acceleration
Nb	Brownian motion parameter	Le	Lewis number
(x, y)	Cartesian coordinates	Nu_x	Nusselt number
T_w	temperature at the plate	Sh_x	Sherwood number
T_∞	ambient temperature attained	u, v	velocity components along $x-y$ axes
T	Temperature on the plate	f_w	Transpiration
Pr	Prandtl number		

The aim of the present paper is to extend the work by Rashidi et al. [40] to the case where the plate is permeable for nanofluids over a cylindrical tube and thermal analysis by DTM- Padé approximation method as powerful analytical method. DTM-Padé is the combination of DTM or differential transformation method as a powerful mathematical method and Padé approximation technique. In recent years, the DTM-Padé has been successfully employed to solve many types of nonlinear problems such as MHD flow in a laminar liquid film [42], nano boundary-layers over stretching surfaces [39], heat transfer in a second-grade fluid through a porous medium [41] and off-centered stagnation flow toward a rotating disc [13].

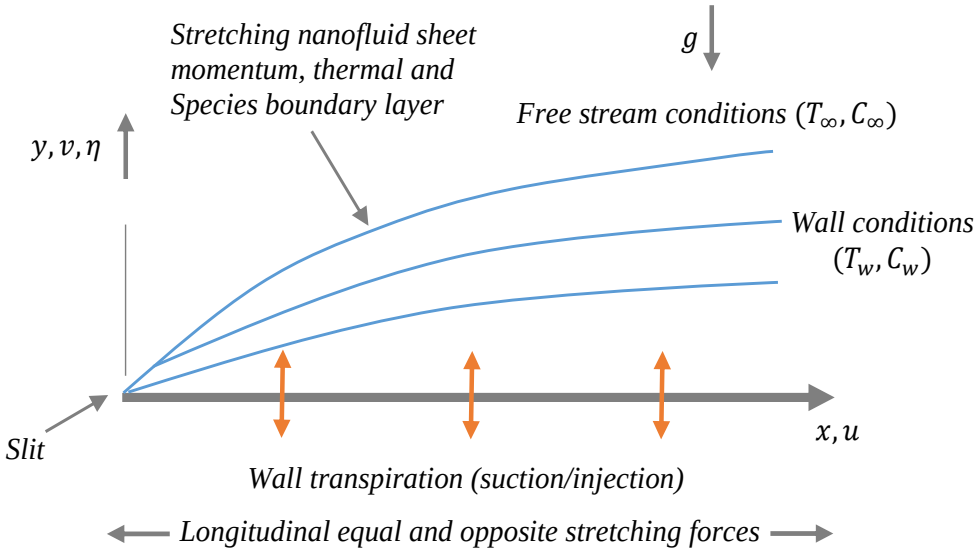

Figure 1: Nanofluid stretching sheet flow physical regime.

2. Mathematical formulation

In this article, we examine steady, incompressible, laminar, boundary layer flow of a nanofluid past a permeable stretching sheet. The simultaneous application of two equal and opposite forces along the x-axis induces flow generation as a result of non-linear stretching of the sheet. The sheet is extended with a velocity $u_w = ax^n$ with the origin location fixed, where the power-law index, n is a nonlinear stretching parameter, a is a constant and x is the coordinate orientated parallel to the stretching surface. Lateral mass flux i.e. wall transpiration is present. The model studied is depicted in Figure 1. This physical regime is of importance in modern nano-technological fabrication and thermal materials processing as elaborated by Krajnik et al. [33]. It is important to note that the constant temperature and concentration of the stretching surface T_w and C_w are assumed to be greater than the ambient temperature and concentration T_∞ and C_∞. The wall conditions are therefore isothermal. Recently, Rana and Bhargava [37] are defined Neglecting buoyancy forces, edge effects, pressure gradient presence and the conservation equations i.e. mass, momentum, energy and nano-particle species conservation equations, following may be presented as

$$\frac{\partial u}{\partial x} + \frac{\partial v}{\partial y} = 0, \tag{2.1}$$

$$u\frac{\partial u}{\partial x}+v\frac{\partial u}{\partial y}=\nu\frac{\partial^2 u}{\partial y^2}, \tag{2.2}$$

$$u\frac{\partial T}{\partial x}+v\frac{\partial T}{\partial y}=\alpha_m \bigtriangledown^2 T+\tau\left[D_B\frac{\partial C}{\partial y}\cdot\frac{\partial T}{\partial y}+(D_T/T_\infty)\left(\frac{\partial T}{\partial y}\right)^2\right], \tag{2.3}$$

$$u\frac{\partial C}{\partial x}+v\frac{\partial C}{\partial y}=D_B\frac{\partial^2 C}{\partial y^2}+(D_T/T_\infty)\frac{\partial^2 T}{\partial y^2}, \tag{2.4}$$

where u and v are the velocity components along the x and y axis, ν is the nanofluid kinematic viscosity, $\alpha_m=k_m/(\rho c)_f$ is the nanofluid thermal diffusivity, $\tau=(\rho c)_p/(\rho c)_f$ is the ratio between the effective heat capacity of the nanoparticles and heat capacity of the base fluid, ρ_p is the density of the nano-particles, ρ_f is the density of the base fluid, D_B is the Brownian diffusion coefficient, D_T is the thermophoretic diffusion coefficient and c is the volumetric volume expansion coefficient. The following boundary conditions are prescribed

$$\begin{aligned}&\text{at } y=0: \quad v=v_w(x), \quad u_w=ax^n, \quad T=T_w, \quad C=C_w,\\ &\text{as } y\to\infty: \quad u=v=0, \quad T=T_\infty, \quad C=C_\infty,\end{aligned} \tag{2.5}$$

where $v_w(x)$ is the variable velocity components in vertical direction at the stretching surface in which $v_w(x)<0$ represents to the suction cases and $v_w(x)>0$ represents to the injection ones. The wall transverse velocity condition in (2.5) differs from that in Rana and Bhargava [37] since wall transpiration is now included. Introducing similarity transformations

$$\eta=y\sqrt{\frac{a(n+1)}{2\nu}}x^{\frac{n-1}{2}}, \quad u=ax^n f'(\eta),$$

$$v=-\sqrt{\frac{a\nu(n+1)}{2}}x^{\frac{n-1}{2}}\left(f+\left(\frac{n-1}{n+1}\right)\eta f'\right),$$

$$\theta(\eta)=\frac{T-T_\infty}{T_w-T_\infty} \quad ,\phi(\eta)=\frac{C-C_\infty}{C_w-C_\infty}.$$

Introduction of these transformations into the governing equations (2.1), (2.2), (2.3), (2.4) yields the reduced form of the conservation equations for momentum, energy (heat) and species (nano-particle) concentration

$$f'''+ff''-\left(\frac{2n}{n+1}\right)f'^2=0, \tag{2.6}$$

$$\frac{1}{pr}\theta''+f\theta'+Nb\theta'\phi'+Nt(\theta')^2=0, \tag{2.7}$$

$$\phi''+\frac{1}{2}Lef\phi'+\frac{Nt}{Nb}\theta''=0. \tag{2.8}$$

The transformed boundary conditions become

$$\eta=0: \quad f=f_w, \quad f'=1, \quad \theta=1, \quad \phi=1, \tag{2.9}$$

$$\eta\to\infty: \quad f'=1, \quad \theta=0, \quad \phi=0, \tag{2.10}$$

where $Pr=\nu/\alpha$ is the Prandtl number, $Nb=(\rho c)_p\times D_B(C_w-C_\infty)/(\rho c)_f\nu$ is the Brownian motion parameter, $Nt=(\rho c)_p D_T(T_w-T_\infty)/(\rho c)_f\nu T_\infty$ is the thermophoresis parameter, $Le=\nu/D_B$ is the Lewis number and $f_w=-v_w(x)/(\sqrt{a\nu(n+1)/2}x^{\frac{n-1}{2}})$ is the wall transpiration parameter (suction/injection). We now march on to find the solution of the boundary value problem (2.6), (2.7), (2.8), (2.9), (2.10) analytically by using DTM-Padé.

3. Analytical approximations by means of the DTM-Padé

By taking the one-dimensional differential transform, from Table 1 to each term of (2.6), (2.7), (2.8), the following transforms are obtained

$$f''' \to (k+1)(k+2)(k+3)F(k+3), \tag{3.1}$$

$$ff'' \to \sum_{r=0}^{k}(k-r+1)(k-r+2)F(r)F(k-r+2), \tag{3.2}$$

$$f'^2 \to \sum_{r=0}^{k}(r+1)F(r+1)(k-r+1)F(k-r+1), \tag{3.3}$$

$$\theta'' \to (k+1)(k+2)\Theta(k+2), \tag{3.4}$$

$$f\theta' \to \sum_{r=0}^{k}F(r)(k-r+1)\Theta(k-r+1), \tag{3.5}$$

$$\theta'^2 \to \sum_{r=0}^{k}(r+1)\Theta(r+1)(k-r+1)\Theta(k-r+1), \tag{3.6}$$

$$\theta'\phi' \to \sum_{r=0}^{k}(r+1)\Theta(r+1)(k-r+1)\Phi(k-r+1), \tag{3.7}$$

$$\phi'' \to (k+1)(k+2)\Phi(k+2), \tag{3.8}$$

$$f\phi' \to \sum_{r=0}^{k}F(r)(k-r+1)\Phi(k-r+1). \tag{3.9}$$

where $F(k)$, $\Theta(k)$, and $\Phi(k)$ are the transformed functions of $f(k)$, $\theta(k)$, and $\phi(k)$ respectively and are given by

$$f(\eta) = \sum_{k=0}^{\infty}F(k)\eta^k, \tag{3.10}$$

$$\theta(\eta) = \sum_{k=0}^{\infty}\Theta(k)\eta^k, \tag{3.11}$$

$$\phi(\eta) = \sum_{k=0}^{\infty}\Phi(k)\eta^k. \tag{3.12}$$

Table 1: The operations for the one-dimensional differential transform method

Original function	Transformed function
$w(x) = u(x) \pm v(x)$	$W(k) = U(k) \pm V(k)$
$w(x) = \lambda u(x)$	$W(k) = \lambda U(k)$, λ is a constant
$w(x) = \frac{du(x)}{dx}$	$W(k) = (k+1)U(k+1)$
$w(x) = \frac{d^r u(x)}{dx^r}$	$W(k) = (k+1)(k+2)\dots(k+r)U(k+r)$
$w(x) = u(x)v(x)$	$W(k) = \sum_{r=0}^{k}U(r)v(k-r)$
$w(x) = \frac{du(x)}{dx}\frac{dv(x)}{dx}$	$W(k) = \sum_{r=0}^{k}(r+1)(k-r+1)U(r+1)V(k-r+1)$
$w(x) = u(x)\frac{dv(x)}{dx}$	$W(k) = \sum_{r=0}^{k}(k-r+1)U(r)V(k-r+1)$
$w(x) = u(x)\frac{d^2u(x)}{dx^2}$	$W(k) = \sum_{r=0}^{k}(k-r+2)(k-r+1)U(r)V(k-r+2)$

By substituting (3.1), (3.2), (3.3), (3.4), (3.5), (3.6), (3.7), (3.8), (3.9) into (2.6), (2.7), (2.8) and by using boundary conditions equations (2.9) and (2.10) we have

$$\begin{aligned}(k+1)(k+2)(k+3)F(k+3)+\sum_{r=0}^{k}F(r)(k-r+2)(k-r+1)F(k-r+2)\\ -\frac{2n}{n+1}\sum_{r=0}^{k}(r+1)F(r+1)(k-r+1)F(k-r+1)=0,\end{aligned} \tag{3.13}$$

$$\begin{aligned}\frac{1}{Pr}(k+1)(k+2)\Theta(k+2)+\sum_{r=0}^{k}F(r)(k-r+1)\Theta(k-r+1)\\ +Nb\sum_{r=0}^{k}(r+1)\Theta(r+1)(k-r+1)\Phi(k-r+1)\\ +Nt\sum_{r=0}^{k}(r+1)\Theta(r+1)(k-r+1)\Theta(k-r+1)=0,\end{aligned} \tag{3.14}$$

$$\begin{aligned}(k+1)(k+2)\Phi(k+2)+\frac{1}{2}Le\sum_{r=0}^{k}F(r)(k-r+1)\Phi(k-r+1)\\ \frac{Nt}{Nb}(k+1)(k+2)\Theta(k+2),\end{aligned} \tag{3.15}$$

$$F(0)=f_w,\quad F(1)=1,\quad F(2)=\alpha, \tag{3.16}$$

$$\Theta(0)=1,\quad \Theta(1)=\beta, \tag{3.17}$$

$$\Phi(0)=1,\quad \Phi(1)=\gamma. \tag{3.18}$$

Moreover, by substituting (3.16), (3.17), (3.18) into (3.13), (3.14), (3.15) and by a recursive method we can calculate the values of $F(k), \Theta(k)$, and $\Phi(k)$.

Hence, by substituting all $F(k), \Theta(k)$, and $\Phi(k)$ into (3.10), (3.11), (3.12), we have the series solutions as below

$$\begin{aligned}f(\eta)\cong f_w+\eta+\alpha\eta^2+\frac{1}{6}\left(\frac{2n}{n+1}-2\alpha f_w\right)\eta^3+\frac{1}{24}\left(-2\alpha-f_w\left(\frac{2n}{n+1}-2\alpha f_w\right)+\frac{8\alpha n}{n+1}\right)\eta^4\\ +\ldots,\end{aligned} \tag{3.19}$$

$$\begin{aligned}\theta(\eta)\cong 1+\beta\eta+\frac{1}{2}Pr\left(-\beta f_w-\beta\gamma Nb+\beta^2-Nt\right)\eta^2+\frac{1}{6}Pr\begin{pmatrix}-\beta-f_wPrA-3\beta NtPrA\\ -\gamma NbPrA-\frac{1}{2}Nb\beta f_wLe\gamma\end{pmatrix}\eta^3\\ +\ldots,\end{aligned} \tag{3.20}$$

$$\begin{aligned}\phi(\eta)\cong 1+\gamma\eta+\frac{1}{2}\left(-\tfrac{1}{2}\gamma f_wLe-\tfrac{NtPrA}{Nb}\right)\eta^2+\frac{1}{6}\begin{pmatrix}-\frac{1}{2}Le\left(f_w\left(-\frac{ANtPr}{Nb}-\frac{\gamma f_wLe}{2}\right)+\gamma\right)\\ -\beta NtPr\left(-\frac{ANtPr}{Nb}-\frac{\gamma f_wLe}{2}\right)+A\gamma NtPr^2\\ \frac{1}{Nb}NtPr\left(-\beta-Af_wPr-2A\beta NtPr\right)\end{pmatrix}\eta^3\\ +\ldots,\end{aligned} \tag{3.21}$$

where $A=\left(-\beta f_w-\beta\gamma Nb-Nt\beta^2\right)$.

Best way to enlarge the convergence radius of the truncated series solution is the Padé approximant where converting the polynomial approximation into a ratio of two polynomials. Without using the Padé

approximant, the analytical solution obtained by the DTM, cannot satisfy boundary conditions at infinity. It is therefore essential to combine the series solution, obtained by the DTM with the Padé approximant to provide an effective tool to handle boundary value problems in infinite domains. Hence apply the Padé approximation to (3.19) and (3.21) and by using asymptotic boundary conditions equations (2.9) and (2.10) at $\eta = \infty$, we can obtain α, β, and γ.

4. Result and discussion

As described in the main aim of this study, the main purpose of current paper is to introduce the DTM as an analytical method for the solution of heat and mass transfer of nanofluid over a stretching plate. Figure 2 demonstrates the accuracy of DTM compared to numerical method.

Table 2: Comparison between the results of DTM-Padé [10,10] and numerical solution, when $f_w = 0, Nt = Nb = 0.5, Pr = 1, n = 1.5$ and $Le = 2$.

	$f'(\eta)$		$\theta(\eta)$		$\phi(\eta)$	
η	DTM-Padé[10,10]	Numerical	DTM-Padé[10,10]	Numerical	DTM-Padé[10,10]	Numerical
0.0	1.000000	1.000000	1.000000	1.000000	1.000000	1.000000
0.5	0.592838	0.592838	0.798988	0.798988	0.843667	0.843667
1.0	0.355768	0.355769	0.600981	0.600981	0.710694	0.710694
1.5	0.215166	0.215169	0.430405	0.430405	0.588966	0.588966
2.0	0.130746	0.130749	0.296400	0.296400	0.475138	0.475138
2.5	0.079650	0.079655	0.197860	0.197860	0.371684	0.371683
3.0	0.048566	0.048572	0.128858	0.128859	0.281979	0.281976
3.5	0.029595	0.029602	0.082282	0.082281	0.207844	0.207828
4.0	0.017992	0.017999	0.051697	0.051687	0.149150	0.149089

As seen in this figure as well as Figures 3, 4, 5 which are depicted for $f(\eta), f'(\eta), \theta(\eta)$ and $\phi(\eta)$, DTM is not a very reliable method for the solution of these kind of the problems which have an infinite boundary condition. As seen in these figures DTM results cannot be converged in infinite and suddenly reaches to

Table 3: Comparison between the results of numerical, DTM-Padé solution and previously published studies [37] and [40], when $f_w = 0, Le = Pr = n = 2$ and $Nb = Nt = 0.5$.

			$f'(\eta)$		
η	FEM	FDM	HAM	Numerical	DTM-Padé
0.0	1.0000	1.0000	1.00000000	1.00000000	1.00000000
1.0	0.3479	0.3459	0.34838179	0.34838043	0.34838006
2.0	0.1270	0.1210	0.12812649	0.12812328	0.12812251
3.0	0.0464	0.0460	0.04815841	0.04815345	0.04815226
4.0	0.0161	0.0160	0.01825518	0.01824889	0.01824752
			$\theta(\eta)$		
η	FEM	FDM	HAM	Numerical	DTM-Padé
0.0	1.0000	1.0000	1.00000000	1.00000000	1.00000000
1.0	0.5016	0.4916	0.47170963	0.47169779	0.47540763
2.0	0.1417	0.1410	0.13847506	0.13845954	0.13991973
3.0	0.0271	0.0270	0.02894668	0.02894410	0.02878420
4.0	0.0043	0.0041	0.00495102	0.00494991	0.00494640

infinite or zero for different profiles. To solve this problem and have accurate results, it is recommended to apply the Padé approximation on the obtained results. Table 2 and Table 3 compares the results of DTM- Padé with the previous numerical and analytical methods presented in the literature. An excellent agreement between these methods can be found in comparison in these tables. So, this order of approximation is used in the following for finding the effect of constant numbers or parameters on the profiles.

The effect of transpiration parameter (for suction and injection conditions) is presented in Figures 6, 7 and 8 for $f'(\eta), \theta(\eta)$ and $\phi(\eta)$, respectively when $Nt = Nb = 0.5, Pr = 1$ and $n = 1.5, Le = 2$. Increasing this parameter makes a decrease in all described graphs due to more injection or suction the fluid. As seen, by increasing this parameter, nanoparticles concentration over the plate will decrease due to more fluid penetration from pores and this is the main reason of lower thermal boundary layer caused by fewer nanoparticles over the plate. Figures 9, 10 and 11 show the influence of sheet stretching parameter on the flow boundary layer, thermal boundary layer and nanoparticles volume fraction concentration. Increase of this parameter can increase the thermal and nanoparticles concentration profile thicknesses while it reduces the flow boundary layer as shown in Figure 9. When the Prandtl number reaches to higher values, thermal boundary thickness reduces due to more heat transfer between the plate and nanofluid as shown in Figure 12. For nanoparticles motion/heat transfer analysis, Brownian motion parameter and thermophoresis parameter have a significant effect on the nanoparticles concentration and thermal boundary layer as presented in Figures 13, 14, 15 and 16. When Brownian motion parameter increases, thermal boundary layer increases while the nanoparticles concentration decreases. Thermophoresis parameter has the same effect on the thermal boundary layer while a diverse effect on the nanoparticles concentration is observed (Figures 15,16). Finally the effect of Lewis number on the thermal and nanoparticles concentration profiles is depicted by Figure 17 and Figure 18, respectively. These figures also confirms that higher Lewis numbers have thinner profiles for both thermal boundary layer and nanoparticles concentration.

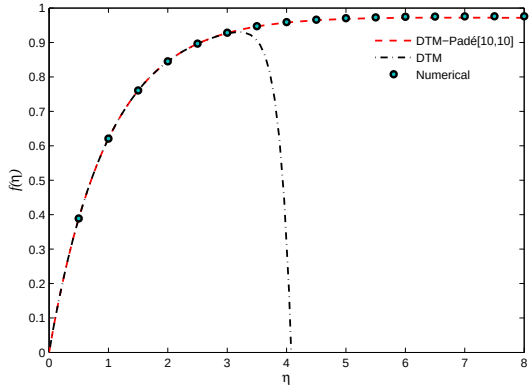

Figure 2: $f(\eta)$ by the DTM and the DTM-Padé [10,10] and comparison with the numerical solution.

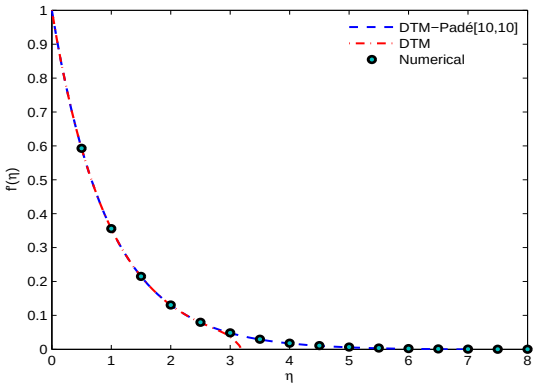

Figure 3: $f'(\eta)$ by the DTM and the DTM-Padé [10,10] and comparison with the numerical solution.

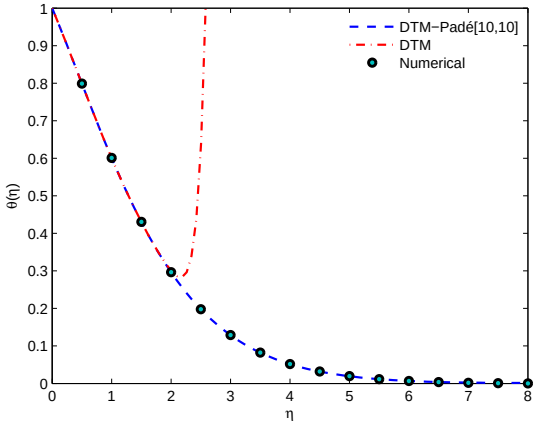

Figure 4: $\theta(\eta)$ by the DTM and the DTM-Padé [10,10] and comparison with the numerical solution.

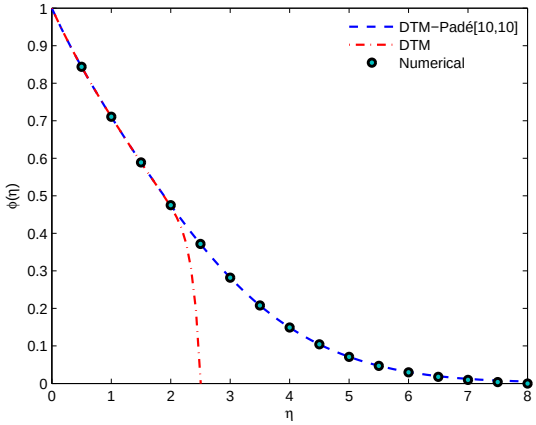

Figure 5: $\phi(\eta)$ by the DTM and the DTM-Padé [10,10] and comparison with the numerical solution.

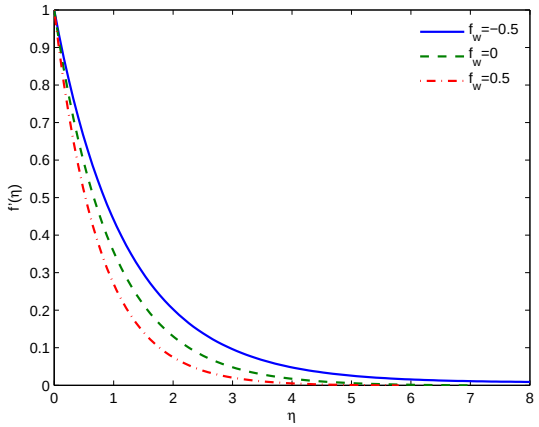

Figure 6: Transpiration (suction/injection) parameter effect on velocity distribution when $Nt = Nb = 0.5, Pr = 1$ and $n = 1.5, Le = 2$.

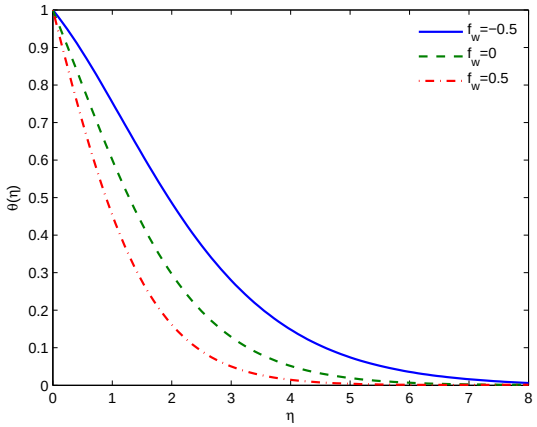

Figure 7: Transpiration (suction/injection) parameter effect on temperature distribution, when $Nt = Nb = 0.5, Pr = 1$ and $n = 1.5, Le = 2$.

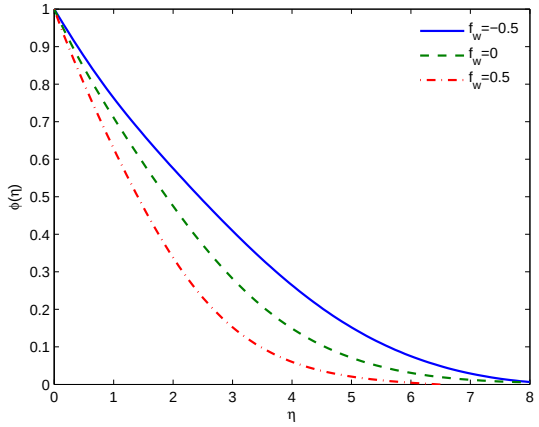

Figure 8: Transpiration (suction/injection) parameter effect on nano-particle concentration distribution, when $Nt = Nb = 0.5, Pr = 1$ and $n = 1.5, Le = 2$.

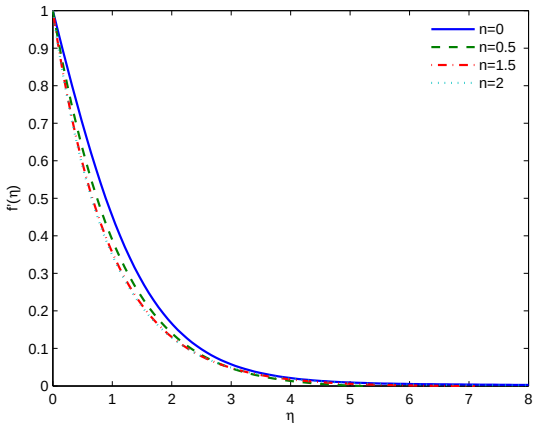

Figure 9: Effect of sheet stretching parameter on velocity distribution, when $f_w = 0, Nt = Nb = 0.5, Pr = 1$ and $Le = 2$.

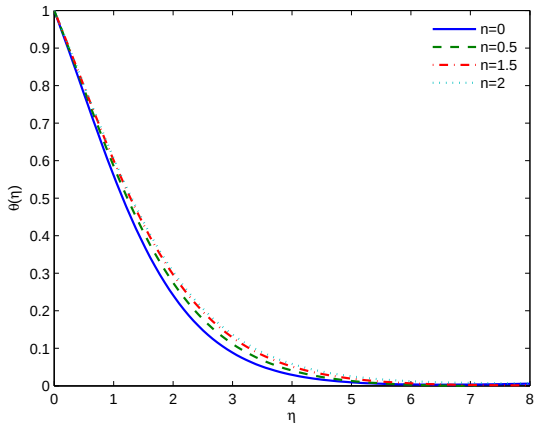

Figure 10: Effect of sheet stretching parameter on temperature distribution, when $f_w = 0, Nt = Nb = 0.5, Pr = 1$ and $Le = 2$.

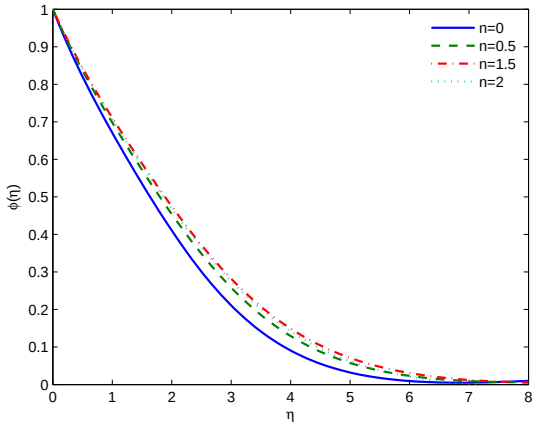

Figure 11: Effect of sheet stretching parameter on nano-particle concentration distribution, when $f_w = 0, Nt = Nb = 0.5, Pr = 1$ and $Le = 2$.

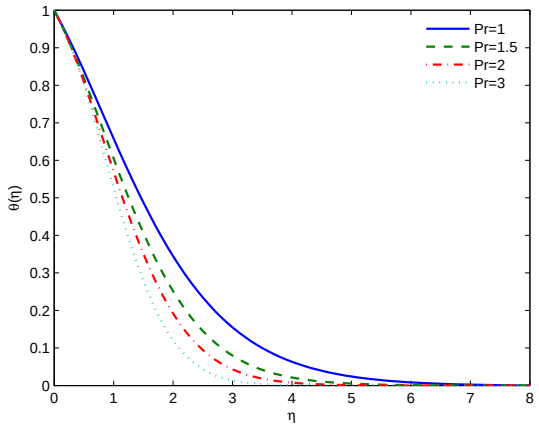

Figure 12: Effect of Prandtl number on temperature distribution when $f_w = 0, Nt = 0.5, Nb = 1, n = 1.5$ and $Le = 2$.

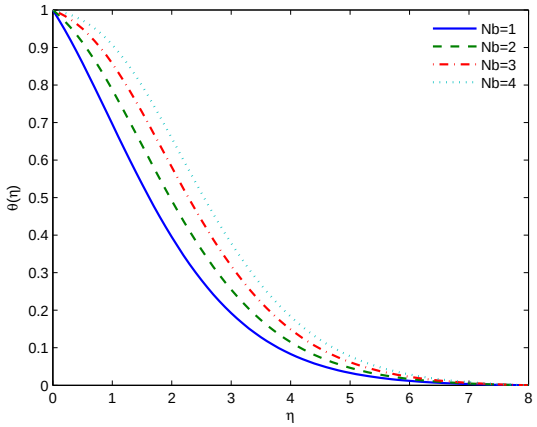

Figure 13: Effect of Brownian motion parameter on temperature distribution when $f_w = 0, Nt = Pr = 1, n = 1.5$ and $Le = 2$.

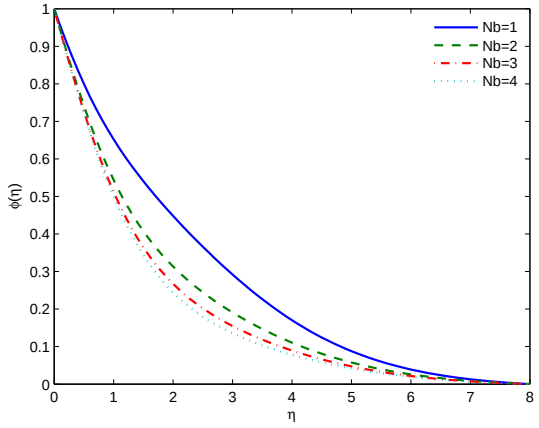

Figure 14: Effect of Brownian motion parameter on nanoparticle concentration distribution when $f_w = 0, Nt = Pr = 1, n = 1.5$ and $Le = 2$.

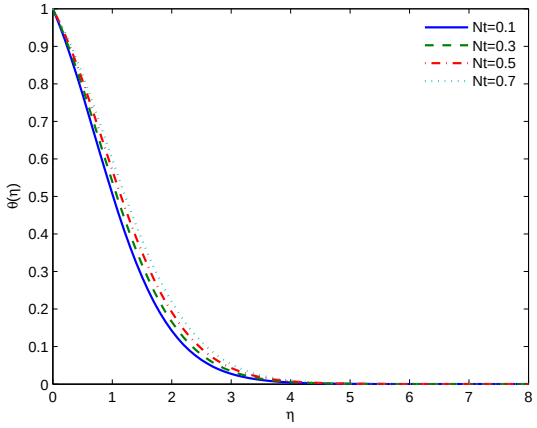

Figure 15: Effect of thermophoresis parameter on temperature distribution when $f_w = 0, Nb = 1, n = 1.5$ and $Pr = Le = 2$.

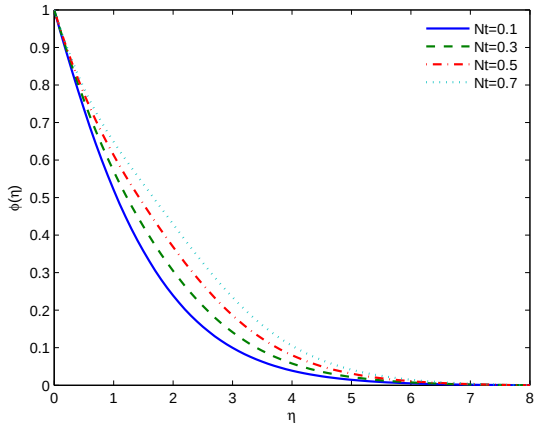

Figure 16: Effect of thermophoresis parameter on nanoparticle concentration distribution when $f_w = 0, Nb = 1, n = 1.5$ and $Pr = Le = 2$.

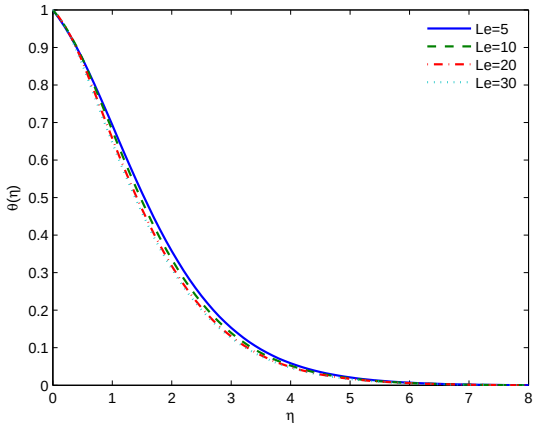

Figure 17: Effect of Lewis number on temperature distribution when $f_w = 0, n = 0.5$ and $Pr = Nb = Nt = 1$.

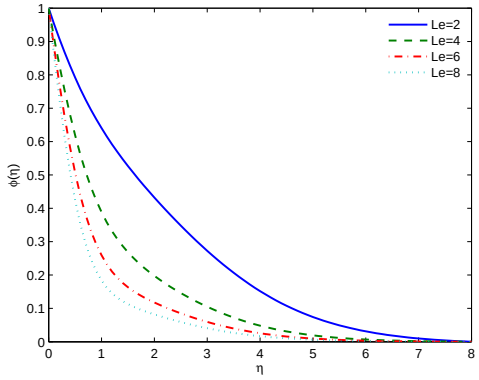

Figure 18: Effect of Lewis number on nano-particle concentration distribution when $f_w = 0, n = 0.5$ and $Pr = Nb = Nt = 1$.

5. Conclusion

In this paper, Differential Transformation Method (DTM) with fourth order Runge-Kutta numerical method have been successfully applied to find the solution of two-phase modeling of heat transfer boundary layer for nanofluids flow over a stretching plate. Due to nonlinearity of governing equations and containing the infinite boundary conditions Padé approximation is applied to solve the problem in higher accuracy. It is found that Padé [10,10] order is the most accurate order of solution. Also, it is tried to find the relation of Prandtl number (Pr), Lewis number (Le) and other parameters such as suction/injection parameter on the thermal boundary layer and nanoparticles volume fraction (ϕ) profile.

References

[1] A. R. Ahmadi, A. Zahmatkesh, M. Hatami, D. D. Ganji, *A comprehensive analysis of the flow and heat transfer for a nanofluid over an unsteady stretching flat plate*, Powder Technol., **258** (2014), 125–133. 1

[2] M. Akbarzadeh, S. Rashidi, M. Bovand, *A sensitivity analysis on thermal and pumping power for the flow of nanofluid inside a wavy channel*, J. Mol. Liq., **220** (2016), 1–13.

[3] N. S. Akber, M. Reza, R. Ellahi, *Influence of induced magnetic field and heat flux with the suspension of carbon nanotubes for the peristaltic flow in a permeable channel*, J. Magn. Magn. Mater., **381** (2015), 405–415.

[4] N. S. Akber, M. Reza, R. Ellahi, *Copper oxide nanoparticles analysis with water as base fluid for peristaltic flow in permeable tube with heat transfer*, Comput. Methods Programs Biomed., **130** (2016), 22–30.

[5] N. S. Akber, M. Reza, R. Ellahi, *Impulsion of induced magnetic field for Brownian motion of nanoparticles in peristalsis*, Appl. Nanosci., **6** (2016), 359–370. 1

[6] A. Aziz, *Heat conduction with Maple*, R.T. Edwards, Philadelphia (PA), (2006). 1

[7] A. S. Dogonchi, M. Hatami, G. Domairry, *Motion analysis of a spherical solid particle in plane Couette Newtonian fluid flow*, Powder Technol., **274** (2015), 186–192. 1

[8] G. Domairry, A. Aziz, *Approximate analysis of MHD squeeze flow between two parallel disks with suction or injection by homotopy perturbation method*, Math. Probl. Eng., **2009** (2009), 17–26. 1

[9] G. Domairry, M. Hatami, *Squeezing Cuwater nanofluid flow analysis between parallel plates by DTM-Padé Method*, J. Mol. Liq., **193** (2014), 37–44. 1

[10] R. Ellahi , H. Hassan, A. Zeeshan, *Shape effects of nanosize particles in CuH2O nanofluid on entropy generation*, Int. J. Heat Mass Transf., **81** (2015), 449–456. 1

[11] R. Ellahi, M. Hassan, A. Zeeshan, *Aggregation effects on water base* Al_2O_3*—nanofluid over permeable wedge in mixed convection*, Asia Pac. J. Chem. Eng., **11** (2016), 179–186. 1

[12] R. Ellahi, M. Hassan, A. Zeeshan, A. A. Khan, *The shape effects of nanoparticles suspended in HFE-7100 over wedge with entropy generation and mixed convection*, Appl. Nanosci., **6** (2016), 641–651. 1

[13] E. Erfani, M. M. Rashidi, A. B. Parsa, *The modified differential transform method for solving off-centered stagnation flow toward a rotating disc*, Int. J. Comput. Methods, **7** (2010), 655–670. 1

[14] M. Fakour, A. Vahabzadeh, D. D. Ganji, M. Hatami, *Analytical study of micropolar fluid flow and heat transfer in a channel with permeable walls*, J. Mol. Liq., **204** (2015), 198–204. 1

[15] S.-Q. Gao, H.-Y. Duan, *Negative norm least-squares methods for the incompressible magnetohydrodynamic equations*, Acta Math. Sci. Ser. B Engl. Ed., **28** (2008), 675–684. 1

[16] S. E. Ghasemi, M. Hatami, G. R. M. Ahangar, D. D. Ganji, *Electrohydrodynamic flow analysis in a circular cylindrical conduit using least square method*, J. Electrostat., **72** (2014), 47–52. 1
[17] S. E. Ghasemi, M. Hatami, D. D. Ganji, *Thermal analysis of convective n with temperature-dependent thermal conductivity and heat generation*, Case Stud. Therm. Eng., **4** (2014), 1–8.
[18] S. E. Ghasemi, M. Hatami, A. K. Sarokolaie, D. D. Ganji, *Study on blood flow containing nanoparticles through porous arteries in presence of magnetic field using analytical methods*, Phys. E Low Dimens. Syst. Nanostruct., **70** (2015), 146–156.
[19] S. E. Ghasemi, P. Valipour, M. Hatami, D. D. Ganji, *Heat transfer study on solid and porous convective fins with temperature-dependent heat generation using efficient analytical method*, J. Cent. South Univ., **21** (2014), 4592–4598.
[20] S. Göektepe, K. Atalık, H. Ertürk, *Comparison of single and two-phase models for nanofluid convection at the entrance of a uniformly heated tube*, Int. J. Therm. Sci., **80** (2014), 83–92. 1
[21] M. Haghshenas Fard, M. Nasr Esfahany, M. R. Talaie, *Numerical study of convective heat transfer of nanofluids in a circular tube two-phase model versus single-phase model*, Int. Commun. Heat Mass Transf., **37** (2010), 91–97. 1
[22] M. Hatami, G. R. M. Ahangar, D. D. Ganji, K. Boubaker, *Refrigeration efficiency analysis for fully wet semi-spherical porous fins*, Energ. Convers. Manage., **84** (2014), 533–540.
[23] M. Hatami, M. C. M. Cuijpers, M. D. Boot, *Experimental optimization of the vanes geometry for a variable geometry turbocharger (VGT) using a Design of Experiment (DoE) approach*, Energ. Convers. Manage., **106** (2015), 1057–1070.
[24] M. Hatami, G. Domairry, *Transient vertically motion of a soluble particle in a Newtonian fluid media*, Powder Technol., **253** (2014), 481–485.
[25] M. Hatami, D. D. Ganji, *Investigation of refrigeration efficiency for fully wet circular porous fins with variable sections by combined heat and mass transfer analysis*, Int. J. Refrig., **40** (2014), 140–151.
[26] M. Hatami, D. D. Ganji, *Motion of a spherical particle in a fluid forced vortex by DQM and DTM*, Particuology, **16** (2014), 206–212.
[27] M. Hatami, D. D. Ganji, *Motion of a spherical particle on a rotating parabola using Lagrangian and high accuracy Multi-step Differential Transformation Method*, Powder Technol., **258** (2014), 94–98.
[28] M. Hatami, D. D. Ganji, *Natural convection of sodium alginate (SA) non-Newtonian nanofluid flow between two vertical flat plates by analytical and numerical methods*, Case Stud. Therm. Eng., **2** (2014), 14–22.
[29] M. Hatami, D. D. Ganji, *Thermal behavior of longitudinal convectiveradiative porous fins with different section shapes and ceramic materials (SiC and Si 3 N 4)*, Ceram. Int., **40** (2014), 6765–6775.
[30] M. Hatami, H. Safari, *Effect of inside heated cylinder on the natural convection heat transfer of nanofluids in a wavy-wall enclosure*, Int. J. Heat Mass Transf., **103** (2016), 1053–1057.
[31] T. Hayat, M. Imtiaz, A. Alsaedi, M. A. Kutbi, *MHD three-dimensional flow of nanofluid with velocity slip and nonlinear thermal radiation*, J. Magn. Magn. Mater., **396** (2015), 31–37. 1
[32] J. A. Khan, M. Mustafa, T. Hayat, A. Alsaedi, *Three-dimensional flow of nanofluid over a non-linearly stretching sheet: an application to solar energy*, Int. J. Heat. Mass. Transf., **86** (2015), 158–164. 1
[33] P. Krajnik, F. Pusavec, A. Rashid, *Nanofluids: Properties, applications and sustainability aspects in materials processing technologies*, Advances in Sustainable Manufacturing, Springer, Berlin, (2011), 107–113. 2
[34] S. T. Mohyud-Din, Z. A. Zaidi, U. Khan, N. Ahmed, *On heat and mass transfer analysis for the flow of a nanofluid between rotating parallel plates*, Aerosp. Sci. Technol, **46** (2015), 514–522. 1
[35] M. N. Ozisik, *Heat conduction*, John Wiley & Sons, New York, (1980).
[36] S. U. Rahman, R. Ellahi, S. Nadeen, Q. Z. Zia, *Simultaneous effects of nanoparticles and slip on Jeffrey fluid through tapered artery with mild stenosis*, J. Mol. Liq., **218** (2016), 484–493. 1
[37] P. Rana, R. Bhargava, *Flow and heat transfer of a nanofluid over a nonlinearly stretching sheet: a numerical study*, Commun. Nonlinear Numer. Simul., **17** (2012), 212–226. 1, 2, 2, 3
[38] S. Rashidi, M. Dehghan, R. Ellahi, M. Riaz, M. T. Jemal-Abad, *Study of stream wise transverse magnetic fluid flow with heat transfer around an obstacle embedded in a porous medium*, J. Magn. Magn. Mater., **378** (2015), 128–137. 1
[39] M. M. Rashidi, E. Erfani, *The modified differential transform method for investigating nano boundary-layers over stretching surfaces*, Internat. J. Numer. Methods Heat Fluid Flow, **21** (2011), 864–883. 1
[40] M. M. Rashidi, N. Freidoonimehr, A. Hosseini, O. A. Bég, T.-K. Hung, *Homotopy simulation of nanofluid dynamics from a non-linearly stretching isothermal permeable sheet with transpiration*, Meccanica, **49** (2014), 469–482. 1, 3
[41] M. M. Rashidi, T. Hayat, T. Keimanesh, H. Yousefian, *A study on heat transfer in a secondgrade fluid through a porous medium with the modified differential transform method*, Heat Transfer-Asian Research, **42** (2013), 31–45. 1
[42] M. M. Rashidi, M. Keimanesh, *Using differential transform method and pad approximant for solving mhd flow in a laminar liquid film from a horizontal stretching surface*, Math. Probl. Eng., **2010** (2010), 14 pages. 1
[43] R. H. Stern, H. Rasmussen, *Left ventricular ejection: model solution by collocation, an approximate analytical method*, Comput. Boil. Med., **26** (1996), 255–261. 1
[44] M. Turkyilmazoglu, *Analytical solutions of single and multi-phase models for the condensation of nanofluid film flow and heat transfer*, Eur. J. Mech. B-Fluid., **53** (2015), 272–277. 1
[45] M. Turkyilmazoglu, *Anomalous heat transfer enhancement by slip due to nanofluids in circular concentric pipes*, Int. J. Heat Mass Transf., **85** (2015), 609–614. 1
[46] A. Zeeshan, A. Majeed, R. Ellahi, *Effect of magnetic dipole on viscous ferro-fluid past a stretching surface with thermal radiation*, J. Mol. Liq., **215** (2016), 549–554. 1